Journal of Computational Mathematics, Vol.19, No.6, 2001, 571–582.

ON THE CENTRAL RELAXING SCHEME II: SYSTEMS OF HYPERBOLIC CONSERVATION LAWS*[1)]

Hua-zhong Tang
(*School of Mathematical Sciences, Peking University, Beijing 100871, China*)
(*LSEC, ICMSEC, Academy of Mathematics and Systems Sciences, Chinese Academy of Sciences, Beijing 100080, China*)

Abstract

This paper continues to study the central relaxing schemes for system of hyperbolic conservation laws, based on the local relaxation approximation. Two classes of relaxing systems with stiff source term are introduced to approximate system of conservation laws in curvilinear coordinates. Based on them, the semi–implicit relaxing schemes are constructed as in [6, 12] without using any linear or nonlinear Riemann solvers. Numerical experiments for one–dimensional and two–dimensional problems are presented to demonstrate the performance and resolution of the current schemes.

Key words: Hyperbolic conservation laws, The relaxing system, The central relaxing schemes, The Euler equations.

1. Introduction

We are interested in construction of the central relaxing schemes for system of nonlinear hyperbolic conservation laws

$$\frac{\partial \mathbf{U}}{\partial t} + \sum_{i=1}^{d} \frac{\partial \mathbf{F}_i(\mathbf{U})}{\partial x_i} = 0, \tag{1.1}$$

with initial data $\mathbf{U}(0, \mathbf{x}) = \mathbf{U}_0(\mathbf{x})$, $\mathbf{x} = (x_1, ..., x_d)$, based on the local relaxation approximation of Eq.(1.1) [2, 3, 6, 8, 9, 12].

To illustrate the basic idea of the relaxing schemes, for the sake of simplicity in the presentation, we restrict our attention to one–dimensional scalar conservation laws

$$\frac{\partial u}{\partial t} + \frac{\partial f(u)}{\partial x} = 0. \tag{1.2}$$

First, introduce a linear hyperbolic system with a stiff source term (hereafter called the *relaxing system*) :

$$\begin{aligned} \frac{\partial u}{\partial t} + \frac{\partial v}{\partial x} &= 0, \\ \frac{\partial v}{\partial t} + a\frac{\partial u}{\partial x} &= -\frac{1}{\epsilon}(v - f(u)), \end{aligned} \tag{1.3}$$

to approximate (1.2), where the small positive parameter ϵ is the relaxation rate, and a is a positive constant satisfying

$$| f'(u) | \leq \sqrt{a}, \quad \forall u \in R. \tag{1.4}$$

* Received April 10, 1997; Final revised March 30, 2000.

[1)] This project supported partly by National Natural Science Foundation of China (No.19901031), the special Funds for Major State Basic Research Projects of China, and the foundation of National key Laboratory of Computational Physics.

In the small relaxation limit $\epsilon \to 0^+$, the relaxing system (1.3) can be approximated to leading order by the following *relaxed* equations

$$v = f(u), \tag{1.5}$$

$$\tfrac{\partial u}{\partial t} + \tfrac{\partial f(u)}{\partial x} = 0. \tag{1.6}$$

The state satisfying (1.5) is usually called the *local equilibrium*. By the Chapman-Enskog expansion [1], we can derive the following first order approximation to (1.3)

$$v = f(u) - \epsilon\{a - [f'(u)]^2\}\tfrac{\partial u}{\partial x}, \tag{1.7}$$

$$\tfrac{\partial u}{\partial t} + \tfrac{\partial f(u)}{\partial x} = \epsilon\tfrac{\partial}{\partial x}(\{a - [f'(u)]^2\}\tfrac{\partial u}{\partial x}). \tag{1.8}$$

It is clear that the above second equation (1.8) is a dissipative approximation to (1.2) under condition (1.4) (which is also referred to as the *subcharacteristic condition* [8]).

The second step is to discrete the relaxing system (1.3) in a proper way (see [6, 7, 12, 13] for details). To avoid the initial layer introduced by the relaxing system (1.3), we can choose the special initial condition for the relaxing system (1.3):

$$\begin{cases} u(x,0) = u_0(x), \\ v(x,0) = v_0(x) \equiv f(u_0(x)). \end{cases} \tag{1.9}$$

In doing so the state is already in equilibrium initially. On the other hand, to avoid any new boundary layers in solving boundary value problems, we can also impose the boundary conditions for v that are consistent to the local equilibrium.

The relaxation limit for systems of conservation laws with a stiff source term was first studied by Liu in [8]. Convergence of solutions of the general relaxing systems are considered later in [2, 3, 9]. Jin and Xin [6] first considered numerical approximations of conservation laws by using the *relaxing systems* and presented a class of nonoscillatory upwind relaxing schemes. Tang and Wu [13] have analyzed a cell entropy inequality of their upwind relaxing schemes. The main advantage of numerically solving the *relaxing systems* (1.3) over the original equation (1.1) lies in its special structures of the linear characteristic fields and localized source term. Numerically solving the *relaxing system* (1.3) enables one to avoid nonlinear Riemann solvers spatially.

Numerical schemes for stiff relaxing systems such as (1.3) were studied in [7]. Proper implicit time discretizations should be taken to overcome the stability constraints brought by the stiff source. Since the source terms in form (1.3) is linear in the variable v, a simple way is to keep the convection terms explicit and the stiff source terms implicit.

However, the numerical experiments have shown that the implementation of their upwind relaxing schemes for general hyperbolic system is more relatively complicated, because of using linear Riemann solvers of a new hyperbolic system with a stiff source term spatially and the choice of a for different problem. Moreover, its cost is too much.

To overcome these drawback and simplify the costly characteristic procedure, we have constructed a class of the central relaxing schemes for scalar conservation laws in [12] without using linear or nonlinear Riemann solvers. The schemes are shown to be TVD (total variation diminishing) and be of the similar relaxed form as one in [6] in the zero relaxation limit For scalar equations, a cell entropy inequality for semidiscrete schemes has also been studied.

This paper continues to study central relaxing schemes for systems of conservation laws, based on using the local relaxation approximation. Two relaxing systems with stiff source term will be introduced for hyperbolic conservation laws in curvilinear coordinates. Numerical experiments for 1D and 2D problems are also presented to demonstrate the performance and resolution of our central relaxing scheme, and in comparison with the upwind relaxing schemes.

The paper is organized as follows. In section 2, we consider the relaxing system with a stiff source term for the general systems of conservation laws in general geometries. In section 3, a class of the central relaxing schemes are constructed. Numerical experiments for 1D and 2D problems are presented and in comparison with the upwind relaxing schemes in section 4.

2. The Relaxing Systems for Systems of Conservation Laws

In this section we introduce the relaxing systems with a stiff source term to approximate the general systems of conservation laws in several space variables.

2.1. One–Dimensional System of Conservation Laws

Consider 1-D systems of conservation laws

$$\frac{\partial \mathbf{U}}{\partial t} + \frac{\partial \mathbf{F}(\mathbf{U})}{\partial x} = 0,\ (x,t) \in R \times R^+,\ \mathbf{U} \in R^m, \tag{2.1}$$

where $\mathbf{F}(\mathbf{U}) \in R^m$ is a smooth vector-valued function. As in the above section, the *relaxing system* can be introduced as

$$\begin{aligned} &\frac{\partial \mathbf{U}}{\partial t} + \frac{\partial \mathbf{V}}{\partial x} = 0,\ \mathbf{V} \in R^m \\ &\frac{\partial \mathbf{V}}{\partial t} + A\frac{\partial \mathbf{U}}{\partial x} = -\frac{1}{\epsilon}(\mathbf{V} - \mathbf{F}(\mathbf{U})),\ \epsilon > 0, \end{aligned} \tag{2.2}$$

where $\mathbf{A}$ is a positive matrix to be chosen. A simple choice of matrix $\mathbf{A}$ is a positive diagonal matrix, i.e.,

$$\mathbf{A} = \mathrm{diag}\{a_1, a_2, ..., a_m\},\ a_k \text{ is constant}, k = 1, 2, \cdots, m.$$

For small ϵ one can also derive the relaxed system for $\mathbf{U}$ as

$$\frac{\partial \mathbf{U}}{\partial t} + \frac{\partial \mathbf{F}(\mathbf{U})}{\partial x} = \epsilon \frac{\partial}{\partial x}(\{\mathbf{A} - [\mathbf{F}'(\mathbf{U})]^2\}\frac{\partial \mathbf{U}}{\partial x}). \tag{2.3}$$

To ensure the dissipative nature of equation (2.3), a subcharacteristic condition is that

$$\mathbf{A} - [\mathbf{F}'(\mathbf{U})]^2 \geq 0, \text{ for all } \mathbf{U} \text{ under consideration.}$$

Remark. Using the Chapman-Enskog expansion, we can also consider the dissipative structure of the first order correction to the original system.

2.2. Multi-Dimensional System of Conservation Laws

For simplicity in the presentation, we only focus on the two–dimensional system of conservation law

$$\frac{\partial \mathbf{U}}{\partial t} + \frac{\partial \mathbf{F}(\mathbf{U})}{\partial x} + \frac{\partial \mathbf{G}(\mathbf{U})}{\partial y} = 0,\ (x,y,t) \in R^2 \times R^+,\ \mathbf{U} \in R^m, \tag{2.4}$$

with initial data

$$\mathbf{U}(0,x,y) = \mathbf{U}_0(x,y). \tag{2.5}$$

where $\mathbf{F}(\mathbf{U}),\ \mathbf{G}(\mathbf{U}) \in R^m$ are two smooth vector-valued functions.

We now change variables in a smooth one to one fasion:

$$\tau = t,\ \xi = \xi(x,y),\ \eta = \eta(x,y). \tag{2.6}$$

The equation becomes

$$\frac{\partial \widetilde{\mathbf{U}}}{\partial t} + \frac{\partial \widetilde{\mathbf{F}}}{\partial \xi} + \frac{\partial \widetilde{\mathbf{G}}}{\partial \eta} = 0, \tag{2.7}$$

where

$$\widetilde{\mathbf{U}} = \mathbf{U}/J,\ \widetilde{\mathbf{F}} = [\xi_x\mathbf{F} + \xi_y\mathbf{G}]/J,\ \widetilde{\mathbf{G}} = [\eta_x\mathbf{F} + \eta_y\mathbf{G}]/J,$$

and the Jacobian of the transformation

$$J = \frac{\partial(\xi,\eta)}{\partial(x,y)} = \xi_x\eta_y - \xi_y\eta_x = 1/(x_\xi y_\eta - x_\eta y_\xi).$$

Then we can introduce two relaxing systems with stiff source term to approximate hyperbolic systems of conservation laws in general geometries.

Method I. The first relaxing system can be introduced to approximate directly equation (2.7) as follows

$$\begin{aligned}
&\frac{\partial\widetilde{\mathbf{U}}}{\partial t} + \frac{\partial\widetilde{\mathbf{V}}}{\partial\xi} + \frac{\partial\widetilde{\mathbf{W}}}{\partial\eta} = 0,\\
&\frac{\partial\widetilde{\mathbf{V}}}{\partial t} + A\frac{\partial\widetilde{\mathbf{U}}}{\partial\xi} = -\frac{1}{\epsilon}(\widetilde{\mathbf{V}} - \widetilde{\mathbf{F}}),\\
&\frac{\partial\widetilde{\mathbf{W}}}{\partial t} + B\frac{\partial\widetilde{\mathbf{U}}}{\partial\eta} = -\frac{1}{\epsilon}(\widetilde{\mathbf{W}} - \widetilde{\mathbf{G}}),\ \epsilon > 0,
\end{aligned} \tag{2.8}$$

where $\widetilde{\mathbf{U}},\ \widetilde{\mathbf{F}},\ \widetilde{\mathbf{G}}$ are defined in (2.7), $\mathbf{A}$ and $\mathbf{B}$ are two positive matrices to be chosen. In this paper we will always assume that matrices $\mathbf{A}$ and $\mathbf{B}$ have the special form $\mathbf{A} = \mathrm{diag}\{a_1, a_2, ..., a_m\}$, $\mathbf{B} = \mathrm{diag}\{b_1, b_2, ..., b_m\}$, a_k and $b_k (k = 1, 2, ..., m)$ are constants.

Method II. A relaxing system is first introduced to approximate equation (2.4)

$$\begin{aligned}
&\frac{\partial\mathbf{U}}{\partial t} + \frac{\partial\mathbf{V}}{\partial x} + \frac{\partial\mathbf{W}}{\partial y} = 0,\\
&\frac{\partial\mathbf{V}}{\partial t} + A\frac{\partial\mathbf{U}}{\partial x} = -\frac{1}{\epsilon}(\mathbf{V} - \mathbf{F}),\\
&\frac{\partial\mathbf{W}}{\partial t} + B\frac{\partial\mathbf{U}}{\partial y} = -\frac{1}{\epsilon}(\mathbf{W} - \mathbf{G}),\ \epsilon > 0,
\end{aligned} \tag{2.9}$$

where $\mathbf{A}$ and $\mathbf{B}$ are two positive matrices to be chosen as above. Then one transforms it into form in curvilinear coordinates

$$\begin{aligned}
&\frac{\partial\widetilde{\mathbf{U}}}{\partial t} + \frac{\partial\hat{\mathbf{V}}}{\partial\xi} + \frac{\partial\hat{\mathbf{W}}}{\partial\eta} = 0,\\
&\frac{\partial\widetilde{\mathbf{V}}}{\partial t} + A\frac{\partial[\xi_x\widetilde{\mathbf{U}}]}{\partial\xi} + A\frac{\partial[\eta_x\widetilde{\mathbf{U}}]}{\partial\eta} = -\frac{1}{\epsilon}(\widetilde{\mathbf{V}} - \widetilde{\mathbf{F}}),\\
&\frac{\partial\widetilde{\mathbf{W}}}{\partial t} + B\frac{\partial[\xi_y\widetilde{\mathbf{U}}]}{\partial\xi} + B\frac{\partial[\eta_y\widetilde{\mathbf{U}}]}{\partial\eta} = -\frac{1}{\epsilon}(\widetilde{\mathbf{W}} - \widetilde{\mathbf{G}}),
\end{aligned} \tag{2.10}$$

where

$$\widetilde{\mathbf{U}} = \mathbf{U}/J,\ \widetilde{\mathbf{V}} = \mathbf{V}/J,\ \widetilde{\mathbf{W}} = \mathbf{W}/J,\ \hat{\mathbf{V}} = \xi_x\widetilde{\mathbf{V}} + \xi_y\widetilde{\mathbf{W}},\ \hat{\mathbf{W}} = \eta_x\widetilde{\mathbf{V}} + \eta_y\widetilde{\mathbf{W}}. \tag{2.11}$$

We refer the reader to [6], where a comprehensive study of the relaxed systems has been presented.

3. The Central Relaxing Schemes for Conservation Laws

In this section we will give the relaxing schemes approximating system of conservation laws.

3.1. The Spatial Discretizations for 1D Conservation Laws

Introduce the spatial grid points $x_j,\ j \in Z$ with the uniform mesh width $\Delta x = x_{j+1} - x_j$, i.e. Δx is a constant, and denote by $w_j(t)$ the approximate point value of w(x,t) at $x = x_j$. The discrete time level are spaced uniformly with the step $\Delta t = t^{n+1} - t^n$ for $n \in Z^+ \cup \{0\}$. In the following we will always assume $\lambda = \frac{\Delta t}{\Delta x}$ a constant. The relaxing schemes are obtained by discreting the system (2.2), for which it is convenient to treat the spatial and time discretization separately .

A spatial discretization to (2.2) in a conservative form can be written as

$$\begin{aligned} &\frac{\partial}{\partial t}\mathbf{U}_j + \frac{1}{\Delta x}(\mathbf{V}_{j+1/2} - \mathbf{V}_{j-1/2}) = 0, \\ &\frac{\partial}{\partial t}\mathbf{V}_j + \frac{\mathbf{A}}{\Delta x}(\mathbf{U}_{j+1/2} - \mathbf{U}_{j-1/2}) = -\frac{1}{\epsilon}\big(\mathbf{V}_j - \mathbf{F}(\mathbf{U}_j)\big), \end{aligned} \tag{3.1}$$

where the numerical flux $\mathbf{U}_{j+1/2}$ and $\mathbf{V}_{j+1/2}$ will be defined in two ways specified below.

Algorithm I.(First order central scheme) The first numerical flux in (3.1) is defined as:

$$\begin{aligned} \mathbf{V}_{j+1/2} &= \frac{1}{2}(\mathbf{V}_{j+1} + \mathbf{V}_j) - \frac{\beta}{2\lambda}(\mathbf{U}_{j+1} - \mathbf{U}_j), \\ \mathbf{U}_{j+1/2} &= \frac{1}{2}(\mathbf{U}_{j+1} + \mathbf{U}_j) - \frac{\beta}{2\mathbf{A}\lambda}(\mathbf{V}_{j+1} - \mathbf{V}_j), \end{aligned} \tag{3.2}$$

where $\beta < 1$ is a constant.

Algorithm II.(Second order MUSCL scheme) The second numerical flux in (3.1) is defined as:

$$\begin{aligned} \mathbf{V}_{j+1/2} &= \frac{1}{2}(\mathbf{V}^R + \mathbf{V}^L) - \frac{\beta}{2\lambda}(\mathbf{U}^R - \mathbf{U}^L), \\ \mathbf{U}_{j+1/2} &= \frac{1}{2}(\mathbf{U}^R + \mathbf{U}^L) - \frac{\beta}{2\mathbf{A}\lambda}(\mathbf{V}^R - \mathbf{V}^L), \end{aligned} \tag{3.3}$$

where

$$\begin{aligned} \mathbf{V}^L &= \mathbf{V}_j + \frac{1}{2}\phi(r_j)\Delta\mathbf{V}_{j+1/2}, \quad \mathbf{V}^R = \mathbf{V}_{j+1} - \frac{1}{2}\phi\left(\frac{1}{r_{j+1}}\right)\Delta\mathbf{V}_{j+1/2}, \\ \mathbf{U}^L &= \mathbf{U}_j + \frac{1}{2}\phi(s_j)\Delta\mathbf{U}_{j+1/2}, \quad \mathbf{U}^R = \mathbf{U}_{j+1} - \frac{1}{2}\phi\left(\frac{1}{s_{j+1}}\right)\Delta\mathbf{U}_{j+1/2}, \\ r_j &= \frac{\mathbf{V}_j - \mathbf{V}_{j-1}}{\mathbf{V}_{j+1} - \mathbf{V}_j}, \qquad s_j = \frac{\mathbf{U}_j - \mathbf{U}_{j-1}}{\mathbf{U}_{j+1} - \mathbf{U}_j}, \end{aligned} \tag{3.4}$$

and $\phi(r)$ is one of some symmetric limiters [11].

Remark. (1) One simple choice of limiters is the so-called minmod limiters

$$\phi(r) = \max(0, \min(1, r)).$$

A sharper limiter was introduced by van Leer [14] as

$$\phi(r) = (\mid r \mid + r)/(1 + \mid r \mid).$$

(2) In fact the above spatial discretizations are using the Lax-Friedrichs type central difference without using linear or nonlinear Riemann solvers. Moreover, the schemes for scalar equation (1.2) have been shown to be TVD(total variation diminishing) and be of the similar relaxed form as in [6] in the zero relaxation limit(see [12]).

3.2. The Spatial Discretizations for 2D Conservation Laws

The extensions of the above spatial discretization for multi-dimensional relaxing systems can be derived in the similar way. In the following we only consider the spatial discretizations

to (2.8).

$$\begin{aligned}
&\frac{\partial}{\partial t}\mathbf{U}_{j,k}+\frac{1}{\Delta x}(\mathbf{V}_{j+1/2,k}-\mathbf{V}_{j-1/2,k})+\frac{1}{\Delta y}(\mathbf{W}_{j,k+1/2}-\mathbf{W}_{j,k-1/2})=0,\\
&\frac{\partial}{\partial t}\mathbf{V}_{j,k}+\frac{\mathbf{A}}{\Delta x}(\mathbf{U}_{j+1/2,k}-\mathbf{U}_{j-1/2,k}) \qquad =-\frac{1}{\epsilon}(\mathbf{V}_{j,k}-\mathbf{F}(\mathbf{U}_{j,k})),\\
&\frac{\partial}{\partial t}\mathbf{W}_{j,k} \qquad +\frac{\mathbf{B}}{\Delta y}(\mathbf{U}_{j,k+1/2}-\mathbf{U}_{j,k-1/2})=-\frac{1}{\epsilon}(\mathbf{W}_{j,k}-\mathbf{G}(\mathbf{U}_{j,k})),
\end{aligned} \tag{3.5}$$

where the numerical flux $\mathbf{U}_{j+1/2,k}$, $\mathbf{U}_{j,k+1/2}$, $\mathbf{V}_{j+1/2,k}$ and $\mathbf{W}_{j,k+1/2}$ will be defined in two ways specified below.

Algorithm I′.(First order central scheme) The first numerical flux in (3.5) is defined as:

$$\begin{aligned}
\mathbf{V}_{j+1/2,k}&=\frac{1}{2}(\mathbf{V}_{j+1,k}+\mathbf{V}_{j,k})-\frac{\beta}{4\lambda}(\mathbf{U}_{j+1,k}-\mathbf{U}_{j,k}),\\
\mathbf{U}_{j+1/2,k}&=\frac{1}{2}(\mathbf{U}_{j+1,k}+\mathbf{U}_{j,k})-\frac{\beta}{4\mathbf{A}\lambda}(\mathbf{V}_{j+1,k}-\mathbf{V}_{j,k}),\\
\mathbf{W}_{j,k+1/2}&=\frac{1}{2}(\mathbf{W}_{j,k+1}+\mathbf{W}_{j,k})-\frac{\beta}{4\lambda}(\mathbf{U}_{j,k+1}-\mathbf{U}_{j,k}),\\
\mathbf{U}_{j,k+1/2}&=\frac{1}{2}(\mathbf{U}_{j,k+1}+\mathbf{U}_{j,k})-\frac{\beta}{4\mathbf{B}\lambda}(\mathbf{W}_{j,k+1}-\mathbf{W}_{j,k}).
\end{aligned} \tag{3.6}$$

Algorithm II′.(Second order MUSCL scheme) The second numerical flux in (3.5) is defined as:

$$\begin{aligned}
\mathbf{V}_{j+1/2,k}&=\frac{1}{2}(\mathbf{V}^{x,R}+\mathbf{V}^{x,L})-\frac{\beta}{4\lambda}(\mathbf{U}^{x,R}-\mathbf{U}^{x,L}),\\
\mathbf{U}_{j+1/2,k}&=\frac{1}{2}(\mathbf{U}^{x,R}+\mathbf{U}^{x,L})-\frac{\beta}{4\mathbf{A}\lambda}(\mathbf{V}^{x,R}-\mathbf{V}^{x,L}),\\
\mathbf{W}_{j,k+1/2}&=\frac{1}{2}(\mathbf{W}^{y,R}+\mathbf{W}^{y,L})-\frac{\beta}{4\lambda}(\mathbf{U}^{y,R}-\mathbf{U}^{y,L}),\\
\mathbf{U}_{j,k+1/2}&=\frac{1}{2}(\mathbf{U}^{y,R}+\mathbf{U}^{y,L})-\frac{\beta}{4\mathbf{B}\lambda}(\mathbf{W}^{y,R}-\mathbf{W}^{y,L}),
\end{aligned} \tag{3.7}$$

where

$$\begin{aligned}
\mathbf{V}^{x,L}&=\mathbf{V}_{j,k}+\frac{1}{2}\phi(r^x_{j,k})\Delta\mathbf{V}_{j+1/2,k}, &\mathbf{V}^{x,R}&=\mathbf{V}_{j+1,k}-\frac{1}{2}\phi\left(\frac{1}{r^x_{j+1,k}}\right)\Delta\mathbf{V}_{j+1/2,k},\\
\mathbf{U}^{x,L}&=\mathbf{U}_{j,k}+\frac{1}{2}\phi(s^x_{j,k})\Delta\mathbf{U}_{j+1/2,k}, &\mathbf{U}^{x,R}&=\mathbf{U}_{j+1,k}-\frac{1}{2}\phi\left(\frac{1}{s^x_{j+1,k}}\right)\Delta\mathbf{U}_{j+1/2,k},\\
\mathbf{W}^{y,L}&=\mathbf{W}_{j,k}+\frac{1}{2}\phi(r^y_{j,k})\Delta\mathbf{W}_{j,k+1/2}, &\mathbf{W}^{y,R}&=\mathbf{W}_{j,k+1}-\frac{1}{2}\phi\left(\frac{1}{r^y_{j,k+1}}\right)\Delta\mathbf{W}_{j,k+1/2},\\
\mathbf{U}^{y,L}&=\mathbf{U}_{j,k}+\frac{1}{2}\phi(s^y_{j,k})\Delta\mathbf{U}_{j,k+1/2}, &\mathbf{U}^{y,R}&=\mathbf{U}_{j,k+1}-\frac{1}{2}\phi\left(\frac{1}{s^y_{j,k+1}}\right)\Delta\mathbf{U}_{j,k+1/2},\\
r^x_{j,k}&=\frac{\mathbf{V}_{j,k}-\mathbf{V}_{j-1,k}}{\mathbf{V}_{j+1,k}-\mathbf{V}_{j,k}}, &s^x_{j,k}&=\frac{\mathbf{U}_{j,k}-\mathbf{U}_{j-1,k}}{\mathbf{U}_{j+1,k}-\mathbf{U}_{j,k}},\\
r^y_{j,k}&=\frac{\mathbf{W}_{j,k}-\mathbf{W}_{j,k-1}}{\mathbf{W}_{j,k+1}-\mathbf{W}_{j,k}}, &s^y_{j,k}&=\frac{\mathbf{U}_{j,k}-\mathbf{U}_{j,k-1}}{\mathbf{U}_{j,k+1}-\mathbf{U}_{j,k}},
\end{aligned} \tag{3.8}$$

and $\phi(r)$ can also be one of some symmetric limiters [11].

3.3 The Time Discretizations

When a stiff relaxing system such as (1.3) was numerically solved, proper implicit time discretizations should be taken to overcome the stability constraints brought by the stiff source

(see [7]). A simple way is to keep the convection terms explicit and the stiff source terms implicit. Since the source terms in form (1.3) is linear in the variable v, we can avoid to solve nonlinear systems of algebraic equation. A general second order Runge-Kutta splitting scheme to (3.1) can be considered

$$\begin{aligned}
&\overline{\mathbf{U}}_j = \mathbf{U}_j^n, && \overline{\mathbf{V}}_j = \mathbf{V}_j^n - \frac{\Delta t}{\epsilon}(\overline{\mathbf{V}}_j - f(\overline{\mathbf{U}}_j)),\\
&\mathbf{U}_j^{(1)} = \overline{\mathbf{U}}_j - \lambda\Delta_+\overline{\mathbf{V}}_{j-1/2}, && \mathbf{V}_j^{(1)} = \overline{\mathbf{V}}_j - a\lambda\Delta_+\overline{\mathbf{U}}_{j-1/2},\\
&\overline{\overline{\mathbf{U}}}_j = \mathbf{U}_j^{(1)}, && \overline{\overline{\mathbf{V}}}_j = \mathbf{V}_j^{(1)} + \alpha\frac{\Delta t}{\epsilon}(\overline{\overline{\mathbf{V}}}_j - f(\overline{\overline{\mathbf{U}}}_j)) + \gamma\frac{\Delta t}{\epsilon}(\overline{\mathbf{V}}_j - f(\overline{\mathbf{U}}_j)),\\
&\mathbf{U}_j^{(2)} = \overline{\overline{\mathbf{U}}}_j - \lambda\Delta_+\overline{\overline{\mathbf{V}}}_{j-1/2}, && \mathbf{V}_j^{(2)} = \overline{\overline{\mathbf{V}}}_j - a\lambda\Delta_+\overline{\overline{\mathbf{U}}}_{j-1/2},\\
&\mathbf{U}_j^{n+1} = \frac{1}{2}(\mathbf{U}_j^n + \mathbf{U}_j^{(2)}), && \mathbf{V}_j^{n+1} = \frac{1}{2}(\mathbf{V}_j^n + \mathbf{V}_j^{(2)}),
\end{aligned} \tag{3.9}$$

where two parameters α and γ should satisfy the consistancy condition: $\alpha + \gamma = -1$. For example $\alpha = +1,\ \gamma = -2$ (see [6]).

Remark. In [12] we have shown that the above central relaxing schemes possess correct relaxation limit in the sense that the zero relaxation limit ($\epsilon \to 0^+$) be a consistent and stable discretization of the the original equation (1.1).

4. Numerical Results

In this section we present some numerical experiments to demonstrate the performance of the above central relaxing schemes, include resolution and entropy-validing. In the following, we will take $\alpha = -1,\ \gamma = 0$ and $\beta = 0.5$ in all cases.

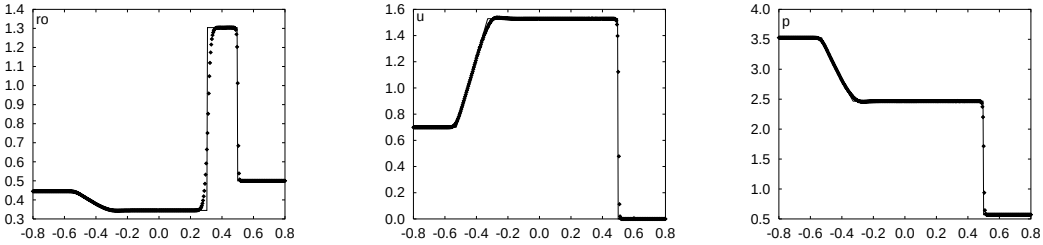

Fig.1. The Lax's shock tube problem tested by the central relaxing schemes, CFL=0.95, t=0.20

4.1. One–Dimensional Test Problems

We consider the 1-D Euler equation of gas dynamics (2.1), where $m = 3$,

$$\mathbf{U} = \begin{pmatrix} \rho \\ \rho u \\ E \end{pmatrix},\ \mathbf{F}(\mathbf{U}) = \begin{pmatrix} \rho u \\ \rho u^2 + p \\ u(E+p) \end{pmatrix}, \tag{4.1}$$

and $p = (\gamma - 1)(E - \frac{1}{2}\rho u^2)$.

Here $\rho,\ u,\ p$ and E are the density,velocity,pressure, and total energy, respectively; $m = \rho u$ is the momentum and we take $\gamma = 1.4$.

We carried out the following 1-D tests .

Example A. The Lax shock tube problem.

Our first set of data is

$$U_L = \begin{pmatrix} 0.445 \\ 0.311 \\ 8.928 \end{pmatrix},\ U_R = \begin{pmatrix} 0.5 \\ 0 \\ 1.4275 \end{pmatrix}. \tag{4.2}$$

The numerical results at $t = 0.20$ shown in Figs. 1 and 2, are obtained by the central relaxing scheme and the upwind relaxing scheme with 500 points under the CFL restriction CFL=0.95. Here we choose $a_1 = 2.4025, a_2 = 11, a_3 = 22.2056$ for the upwind relaxing scheme, $a_1 = a_2 = a_3 = 1.0$ for the central relaxing scheme, and $\epsilon = 10^{-8}$ as in [6].

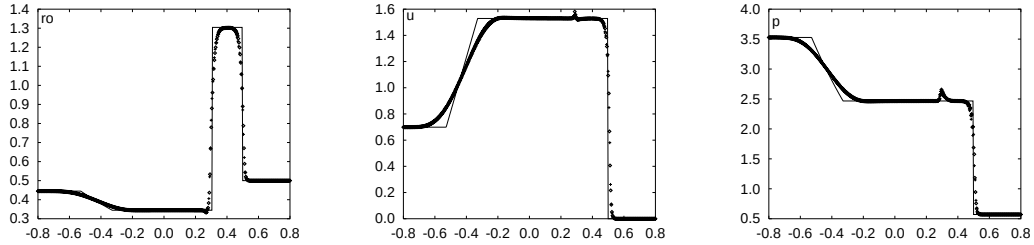

Fig.2. The Lax's shock tube problem tested by the upwind relaxing schemes, CFL=0.95, t=0.20

Example B. The Sod shock tube problem.

Our second set of data is

$$U_L = \begin{pmatrix} 1.0 \\ 0.0 \\ 2.5 \end{pmatrix}, \; U_R = \begin{pmatrix} 0.125 \\ 0.0 \\ 0.25 \end{pmatrix}. \tag{4.3}$$

The numerical results at $t = 0.20$ shown in Figs. 3 and 4, are obtained by the central relaxing scheme and the upwind relaxing scheme with 500 points. In this problem we take $a_1 = 1, a_2 = 1.68, a_3 = 5.045, cfl = 0.95$ and $\epsilon = 10^{-8}$ as in [6].

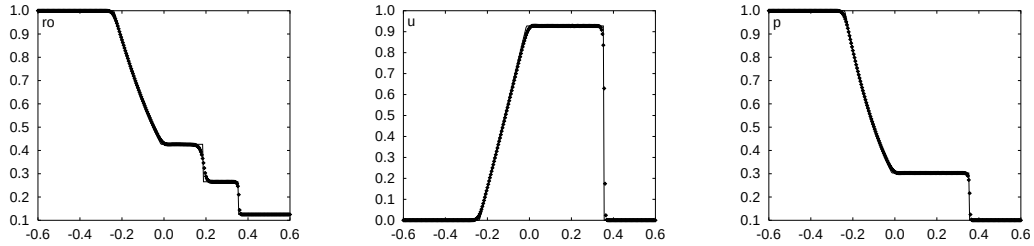

Fig.3. The Sod's shock tube problem tested by the central relaxing schemes, CFL=0.95, t=0.20

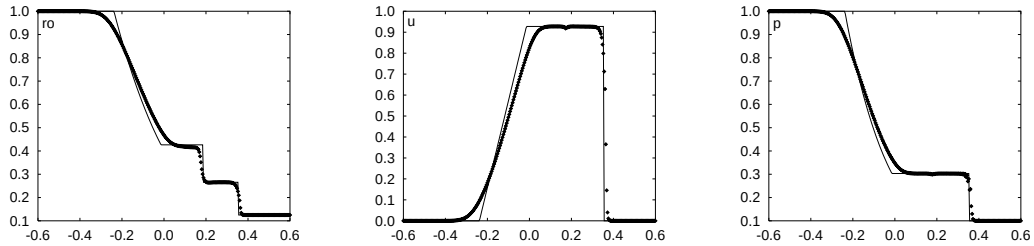

Fig.4. The Sod's shock tube problem tested by the upwind relaxing schemes, CFL=0.95, t=0.20

Remark. (1) In Figs. 1–4, "$\diamond$" and "+" represent the numerical solutions of the relaxing schemes with minmod slope limiter and van Leer slope limiter, respectively. The exact solution is shown by the solid lines. We can observe that all schemes give correct solution. But, the central scheme does much better than the upwind scheme at corners of rarefactions(discontinuities in derivatives), contact discontinuity and shock.

(2) Our central schemes is independent of the choice of matrix **A**. The better resolution can be obtained when the smaller value of $a_i (i = 1, 2, 3)$ is used. But one should be give more care to the choice of matrix **A** for different problem to keep numerical stability when using the upwind relaxing scheme.

Example C. Interaction of Blast Waves[5, 15]

Here we present numerical experiments with the MUSCL-type relaxing scheme for the problem:

$$U(x,0) = \begin{cases} U_L, & 0 \le x < 0.1, \\ U_M, & 0.1 \le x < 0.9, \\ U_R, & 0.9 \le x < 1, \end{cases} \tag{4.4}$$

where

$$\rho_L = \rho_M = \rho_R = 1,\ u_L = u_M = u_R = 0,\ p_L = 1000,\ p_M = 0.01,\ p_R = 100, \tag{4.5}$$

the boundaries at $x = 0$ and $x = 1$ are solid walls. This problem was suggested by Woodward and Colella[15] as a test problem.

In our calculations we divided the interval (0,1) into N cells by

$$x_j = (j - \frac{1}{2})/N,\ j = 1, ..., N, \tag{4.6}$$

where x_j marks the center of the jth cell. The boundary conditions of a solid wall in $x = 0$ and $x = 1$ were treated by reflection [5].

In Figs. 5–6 we show the solution of the MUSCL-type scheme with van Leer slope limiter at $t = 0.038$, respectively. The solid lines are numerical solution of MUSCL-type central relaxing scheme with van Leer slope limiter and 2000 points. "$\diamond$" represents the numerical solutions of the relaxing schemes with van Leer slope limiter and 800 points.

The MUSCL-type central relaxing scheme captures important structures on the fine grid and the results are comparable to other high resolution schemes in [5, 15].

We refer the reader to [5, 15], where a comprehensive comparison of the performance of various schemes for this problem is presented, and a highly accurate solution is displayed and a detailed description of the various interactions that occur at these instances is presented.

In this problem we take $a_1 = 0.1, a_2 = 0.2, a_3 = 0.3$ and $\epsilon = 10^{-8}$ for central schemes, and $a_1 = 500, a_2 = 500, a_3 = 500$ and $\epsilon = 10^{-8}$ for upwind schemes.

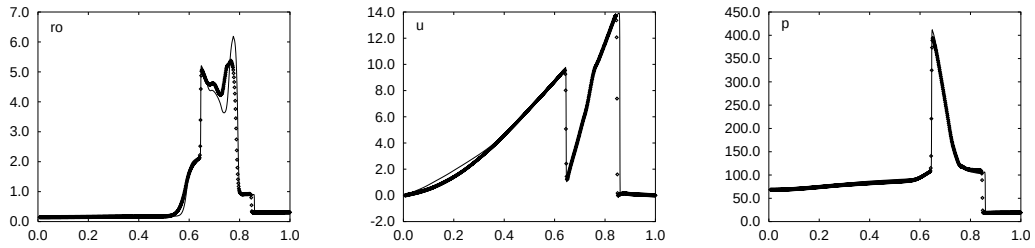

Fig.5. Interaction of Blast Waves tested by the central relaxing schemes

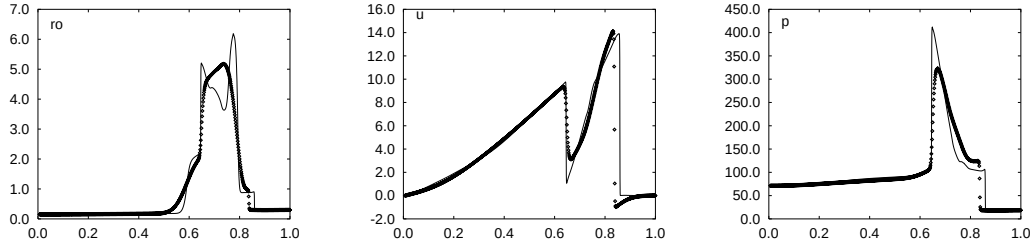

Fig.6. Interaction of Blast Waves tested by the upwind relaxing schemes

4.2. Two–Dimensional Test Problems

We consider the 2D Euler equation of gas dynamics (2.4), where $m = 4$,

$$\mathbf{U} = \begin{pmatrix} \rho \\ \rho u \\ \rho v \\ E \end{pmatrix}, \ \mathbf{F}(\mathbf{U}) = \begin{pmatrix} \rho u \\ \rho u^2 + p \\ \rho uv + p \\ u(E+p) \end{pmatrix}, \ \mathbf{G}(\mathbf{U}) = \begin{pmatrix} \rho v \\ \rho uv + p \\ \rho v^2 + p \\ v(E+p) \end{pmatrix}, \tag{4.7}$$

and $p = (\gamma - 1)(E - \frac{1}{2}\rho(u^2 + v^2))$. Here $\rho,\ u,\ v$, p and E are the density,velocity,pressure, and total energy, respectively; $m = \rho u, n = \rho v$ is the momentum and we take $\gamma = 1.4$.

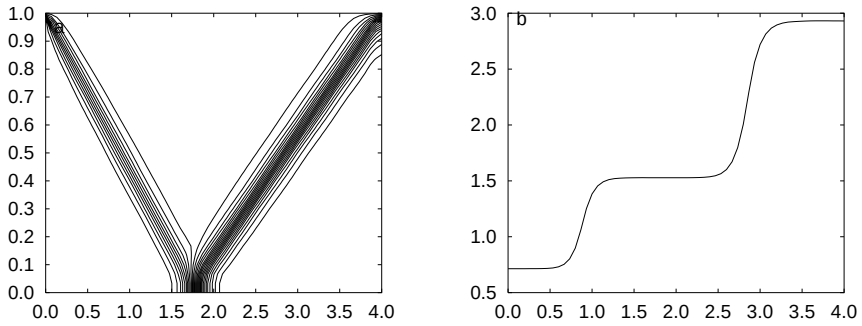

Fig.7. Regular shock reflection. (a) Pressure contour. (b) Pressure profile along the line $y = 0.525$.

Example D. Regular shock reflection.

The computational domain is a rectangle of length 4 and height 1 divided into $M \times N$ rectangular grids with $\Delta x = 1/(M-1)$ and $\Delta y = 1/(N-1)$. Dirichlet conditions are imposed on the left and upper boundaries as

$$(\rho,\ u,\ v, p) =|_{0,y,t}= (1, 2.9, 0, 0.714286),$$
$$(\rho,\ u,\ v, p) =|_{x,1,t}= (1.69997, 2.61934, -0.50633, 1.52919),$$

The bottom boundary is a reflecting wall and the supersonic outflow condition is applied along the right boundary. Initially,the entire flow field is set equal to the free stream supersonic inflow values. Our results obtained by using the MUSCL-type relaxing scheme have shown in Fig.7 with $\beta = 0.5$. Here 30 equally distributed pressure contours are shown. In this problem we take $a_1 = a_2 = a_3 = a_4 = 3.74118, b_1 = b_2 = b_3 = 1.62810$ and $\epsilon = 10^{-8}$. A uniform mesh of 30×60 in the computational domain is used.

Example E. Flow past a cylinder [10].

Finally, we turn our attention to the two dimensional flow past a circular cylinder with a free stream Mach number of 3.0. In the physical space, a cylinder of unit radius is positioned at the origin on a $x - y$ plane. There is a smooth one to one fasion:

$$\begin{aligned} x &= x(\xi, \eta) = (R_x - (R_x - 1)\xi)\cos(\theta(2\eta - 1)), \\ y &= y(\xi, \eta) = (R_y - (R_y - 1)\xi)\sin(\theta(2\eta - 1)), \end{aligned} \tag{4.8}$$

between the computational domain and the physical domain. The computational domain is chosen to be $[0,1] \times [0,1]$ on $\xi - \eta$ plane, which includes bow shock in its interior. We take $R_x = 3$, $R_y = 6$, and $\theta = \frac{5\pi}{12}$. Reflective boundary condition is imposed at the surface of the cylinder,i.e., $\xi = 1$, inflow boundary condition is applied at $\xi = 0$ and outflow boundary condition is at $\eta = 0, 1$. The mesh in the physical space has shown in Fig.8. Our results obtained by using the MUSCL-type relaxing scheme have shown in Figs.8 and 9, based the relaxing models (2.8) and (2.10), respectively. Here 20 equally distributed pressure contours are shown. In this problem we take $a_1 = a_2 = a_3 = a_4 = 3.74118, b_1 = b_2 = b_3 = 1.62810$, and $\beta = 0.5$. In Fig.8, "$\diamond$" and "$+$" represent the numerical solutions of the relaxing schemes with model (2.8) and (2.10) ,respectively. Here uniform meshes of 120×160 and 60×80 in the computational domain are used for models (2.8) and (2.10), respectively.

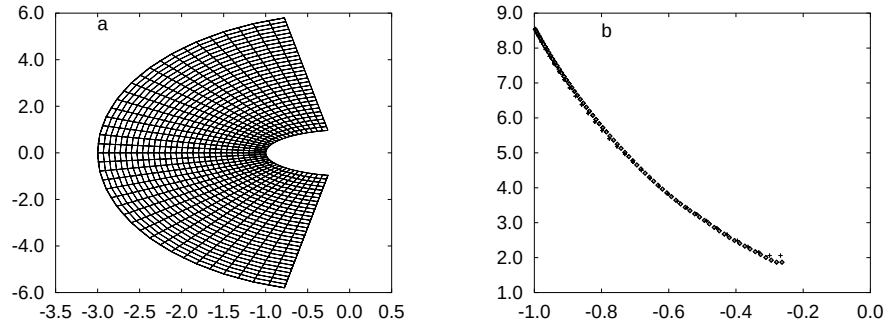

Fig.8. Flow past a cylinder. (a) The mesh. (b) Surface pressure distribution.

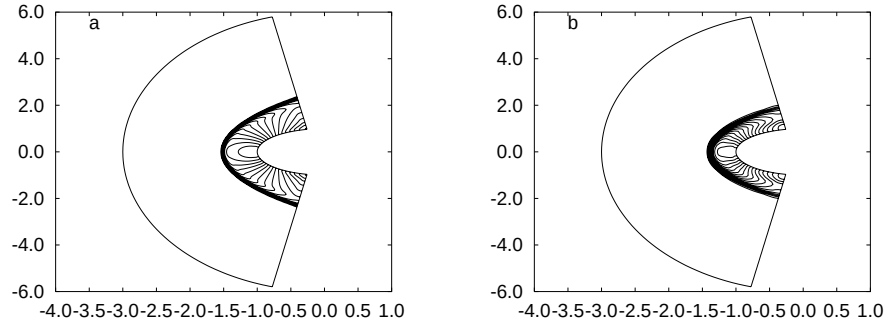

Fig.9. Pressure contour for supersonic flow past a cylinder. (a) Model (2.8). (b) Model (2.10).

References

[1] S. Chapman, T.G. Cowling, The Mathematical Theory of Nonuniform Gases, 3rd Edition, Cambridge Univ. Press, 1970.

[2] G.Q. Chen, T.P. Liu, Zero relaxation and dissipation limits for hyperbolic conservation laws, *Comm. Pure Appl. Math.,* **46** (1993), 755–781.

[3] G.Q. Chen, C.D. Levermore, T.P. Liu, Hyperbolic conservation laws with stiff relaxation terms and entropy, *Comm. Pure Appl. Math.,* **47** (1994), 787–830.

[4] A. Harten, High resolution schemes for hyperbolic conservation laws, *J. Comput. Phys.,* **49** (1983), 357–393.

[5] A. Harten, B. Engquist, S. Osher, S.R. Chakravarthy, Uniformly high order accurate essentially non-oscillatory schemes, III, *J. Comput. Phys.,* **71** (1987), 231–303.

[6] S. Jin, Z.P. Xin, The relaxing schemes for systems of conservation laws in arbitrary space dimensions, *Comm. Pure Appl. Math.,* **48** (1995), 235–281.

[7] S. Jin, Runge–Kutta methods for hyperbolic conservation laws with stiff relaxation terms, *J. Comput. Phys.,* **122** (1995), 51–67.

[8] T.P. Liu, Hyperbolic conservation laws with relaxation, *Comm. Math. Phys.,* **108** (1987), 153–175.

[9] R. Natalini, Convergence to equilibrium for the relaxation approximations of conservation laws, *Comm. Pure and Appl. Math.,* **49** (1996), 795–824.

[10] S. Osher, S. Chakravarthy, Upwind schemes and boundary conditions with applications to Euler equations in general geometries, *J. Comput. Phys.,* **50** (1983), 447–481.

[11] P.R. Sweby, High resolution schemes using flux limiters for hyperbolic conservation laws, *SIAM J. Numer. Anal.,* **21** (1984), 995–1011.

[12] H.Z. Tang, On the central relaxing scheme I: Single conservation laws, *J. Comput. Math.,* **18** (2000), 313–324.

[13] H.Z. Tang, H.M. Wu, On a cell entropy inequality for the relaxing schemes for scalar conservation laws, *J. Comput. Math.,* **18** (2000), 69–74.

[14] B. van Leer, owards the ultimate conservative difference schemes V. A second-order sequal to Godunov's method, *J. Comput. Phys.,* **32** (1979), 101–136.

[15] P. R. Woodward, P. Colella, The numerical Simulation of two-dimensional fluid flow with strong shocks, *J. Comput. Phys.,* **54** (1984), 115–173.